

PAPER • OPEN ACCESS

## Theoretical and experimental modal analysis of circular cross-section shaft

To cite this article: Yahya Muhammed Ameen and Jaafar Khalaf Ali 2020 *IOP Conf. Ser.: Mater. Sci. Eng.* **745** 012066

View the [article online](#) for updates and enhancements.



The banner features a background of a globe with a grid overlay. On the left, there are three circular logos: the top one is 'ECS' in a circle, the middle one is 'The Electrochemical Society' with a stylized 'ECS' logo, and the bottom one is 'THE KOREAN ELECTROCHEMICAL SOCIETY'. The main text in the center reads 'Joint International Meeting PRiME 2020 October 4-9, 2020' in white and blue. Below this, a blue bar contains the text 'Attendees register at NO COST!' in white. On the right side, there is a large blue logo for 'PRiME' with 'PACIFIC RIM MEETING ON ELECTROCHEMICAL AND SOLID STATE SCIENCE' underneath, and '2020' in large white numbers. At the bottom right, a blue bar contains the text 'REGISTER NOW' with a white arrow pointing right.

# Theoretical and experimental modal analysis of circular cross-section shaft

Yahya Muhammed Ameen<sup>\*1</sup> and Jaafar Khalaf Ali<sup>2</sup>

<sup>1,2</sup>Dept. of Mechanical Engineering, College of Engineering, University of Basrah, Basrah, Iraq

\* yahyaameen@yahoo.com

**Abstract.** Experimental Modal Analysis (EMA) is very helpful in engineering design and manufacturing of machine components. In this paper, modal parameters which are natural frequencies, mode shapes and damping ratios are extracted for free-free boundary conditions circular shaft, using EMA, then two disks are added to this shaft as second case study. EMA has been verified as effective and accurate tool, despite of increasing geometrical complexity and nonlinear behaviour of the structure. The two well-known excitation techniques (i.e. impact hammer and shaker) are used for this purpose. For validation, natural frequencies and mode shapes are determined analytically and numerically by Finite Element Modelling (FEM) ANSYS 15 workbench software, and then compared with results obtained experimentally. Noticeable remarks about these approaches are listed. Coherence plots are compared between impact and shaker tests. Digital Signal Processing (DSP) settings like windows type and sample (record) time are compared. The recommended DSP settings mentioned in this work can be used as a general guidance for researchers and people who are working in modal analysis.

**Keywords:** experimental modal analysis, frequency response function, modal parameters, coherence, processing windows.

## 1. Introduction

In order to understand vibrational behaviour and avoid (or control) vibrational problems, researchers and engineers often resort to effective and reliable tool called Experimental Modal Analysis (EMA). The basic idea of EMA is exciting the structure under test mechanically via impact hammer (impulse force) or shaker (periodic and/or random forces), then the dynamic response (acceleration, velocity or displacement) due to this excitation measured simultaneously. After data transformation of the two signals from time domain to frequency domain, analysing these signals leads to evaluation of Frequency Response Function (FRF), a cornerstone of modal analysis. The most important results are modal parameters (so called dynamic characteristics), which are natural frequencies, modal damping and mode shapes (characteristic displacement patterns).

Beginning from 1940's (e.g. Kennedy and Panu [1]), EMA used increasingly and had become considerable approach to evaluate modal parameters of static and dynamic structures in mechanical and civil engineering design and in health monitoring. EMA related strongly with Digital Signal Processing (DSP) techniques. Generation of FRF's requires adequate (or correct) DSP settings (Richard C. and James [2], Peter Avitabile [3]).

Modal parameters of rotating structures are functions of rotational speed. This complexity together with the nature of moving parts, make it difficult to apply EMA on rotating structures. Special instruments and knowledge are required to get accurate results. However, there is no significant



change in modal parameters when the gyroscopic effects are negligible, as in light weight, low damping, and low rotational speed structures, which are the case in wide range of applications, Manoj et al [4].

Circular cross-sectional shaft is essential part in rotor assembly, so, it is important to understand its vibrational behaviour. This task can be successfully performed by employing EMA, which is the main objective of this paper.

Songmao et al [5] used focused acoustic transducer (FUT) force as non-contact excitation. This method is effective with small and lightweight structures like microelectromechanical systems (MEMS) cantilever and thumb nail size turbine blade. Sadeghi et al [6], hanged turbo-pump shaft vertically (along its symmetric axis) using hook and low stiffness glue, to give free-free condition mounting. They found that signal to noise ratio improved considerably in comparison with classical horizontal suspending method. In Luis et al [7] work, natural frequencies and mode shapes of turbo compressor shaft are extracted by EMA and used as input values to FEA model. The shaft divided into 6 elements. In the equation of motion, the displacement vector is filled with experimental data for unitary force vector. Then, unknown stiffness and mass in the model can be calculated to build dynamic FEA model. The shaft tested virtually using this model. Good agreement shown between their model and experimental results. Pramod K. et al [8] tested the effect of crack location and depth on the dynamic behavior of beams. It is known that all natural frequencies are affected by crack existence. However, they found that when the crack positioned near the fixed end of beam, the first natural frequency is mostly affected, but the second natural frequency is mostly affected when the crack at the center of beam, and so on for higher modes.

Coherence function reflects the causal and linear relationship between the output  $x(t)$  and input  $f(t)$ , [9]. High quality FRF and coherence function is crucial in finding accurate estimation of modal parameters, Ashory M. R. [10]. In spite of importance of this indicator, it is neglected mostly in research works related to EMA. Coherence function will be included in this work.

Structural steel solid shaft of 600 mm length and 19 mm diameter is taken as a case study. Material properties of the shaft are: mass density  $\rho=7850$  kg/m<sup>3</sup>, Modulus of elasticity  $E=200$  MPa and Poisson's ratio  $\nu=0.3$ .

A case of free-free boundary conditions shaft is chosen, then experimentally determined natural frequencies and mode shapes are compared -for validation- with those found analytically and numerically. Good agreement was noticed between experimental and theoretical results.

In general, shafts in rotors (like those used in electric motors, turbines, helicopters, etc.) contain other disk-like mechanical elements to perform the required work. These elements are often having complex geometry, and cannot be easily simulated to accurately estimate their natural frequencies and mode shapes, so it can be substituted by equivalent solid disks. In this work, two Aluminum disks will be added to the shaft to examine the efficiency of EMA.

It is seldom to find papers that give sufficient details about handling with EMA. In this paper, essential DSP settings and types of windows in excitation and response will be specified. In this work, importance of windows type and impact sample time selection will be explained.

## 2. Analytical modal analysis

The tested shaft in this work can be considered as horizontal slender cylindrical beam with uniformly distributed mass, subjected to forces applied perpendicularly to the axis of the shaft. Basically, Bernoulli-Euler-Timoshenko beam theory supposed that any plane cross-section of slender beams remains plane and normal to the longitudinal axis during small bending. This assumption simplifies the solution of the equation of motion to extract the natural frequencies and mode shapes of the shaft under study [11].

Depending on the theory mentioned above, and applying free-free boundary conditions in the modal solution of the equation of motion, provides the natural frequencies:

$$f_i = \frac{\lambda_i^2}{2\pi l^2} \sqrt{\frac{E I_z}{m}}, \text{ Hz, } i=1,2,3, \dots \quad (1)$$

Where  $E$ ,  $I_z$  and  $m$  are: modulus of elasticity, area moment of inertia of cross section about z-axis through the centroid and mass per unit length respectively. Mode shapes are:

$$\tilde{y}_i\left(\frac{\lambda_i x}{L}\right) = \cosh\frac{\lambda_i x}{L} + \cos\frac{\lambda_i x}{L} - \sigma_i \left(\sinh\frac{\lambda_i x}{L} + \sin\frac{\lambda_i x}{L}\right) \quad (2)$$

Where  $x$  and  $\tilde{y}$  are axial coordinate and lateral displacement respectively. Values of  $\lambda_i$  and  $\sigma_i$  are given in Table 1 [11].

**Table 1.** Values of  $\lambda_i$  and  $\sigma_i$  in equation 2.

i	$\lambda_i$	$\sigma_i$
1	4.7300	0.98250
2	7.8532	1.00078
3	10.996	0.99997

Generally, damping in each mode cannot be predicted from theoretical models [12]. Therefore, in this work, natural frequencies and mode shapes will be compared among analytical, numerical, and experimental results, but damping comparison will not be performed.

### 3. NUMERICAL MODAL ANALYSIS

Using ANSYS software, finite element analysis (FEA) is carried out on the shaft under study, utilizing built in modal analysis tool. Default mesh settings of the three-dimensional model, were kept without changes, considering natural frequencies and mode shapes related to bending modes only.

### 4. EXPERIMENTAL MODAL ANALYSIS

Measuring both the external force applied to the structure and resulting response, leads to deduction of frequency response functions (FRF) and then modal parameters. This is the principle idea of experimental modal analysis or modal testing. EMA consider linear and time invariant systems.

The equation of motion of viscously damped forced multi degree of freedom system is given by [9]:

$$\mathbf{M}\{\ddot{x}\} + \mathbf{C}\{\dot{x}\} + \mathbf{K}\{x\} = \{f(t)\} \quad (3)$$

Where  $x(t)$  describing the displacement due to the applied force  $f(t)$ ,  $\mathbf{M}$  is the mass matrix,  $\mathbf{C}$  is the damping matrix, and  $\mathbf{K}$  is the stiffness matrix. The Laplace transform of the above equation is:

$$[\mathbf{M} s^2 + \mathbf{C} s + \mathbf{K}] \{X(s)\} = \{F(s)\} \quad (4)$$

The dynamic stiffness matrix is  $\mathbf{Z}(s) = [\mathbf{M} s^2 + \mathbf{C} s + \mathbf{K}]$

Receptance matrix is  $\alpha(s) = \frac{\{X(s)\}}{\{F(s)\}} = \mathbf{Z}(s)^{-1} = [\mathbf{M} s^2 + \mathbf{C} s + \mathbf{K}]^{-1}$

$$\{X(s)\} = \alpha(s)\{F(s)\} = \begin{bmatrix} \alpha_{11}(s) & \alpha_{12}(s) & \dots \\ \alpha_{21}(s) & \alpha_{22}(s) & \\ \vdots & & \end{bmatrix} \{F(s)\} \quad (5)$$

Where  $\alpha_{ij}(s)$  relates the response at node  $i$  with the only force at node  $j$ .

$$\alpha(s) = [\mathbf{M} s^2 + \mathbf{C} s + \mathbf{K}]^{-1} = \frac{adj(\mathbf{M} s^2 + \mathbf{C} s + \mathbf{K})}{det(\mathbf{M} s^2 + \mathbf{C} s + \mathbf{K})} \quad (6)$$

When the damping is small, the roots of the characteristic polynomial equation in the numerator are complex conjugate pole pairs,  $\lambda_r$  and  $\lambda_r^*$ ,  $r = 1, 2, \dots, N$ , with  $N$  the number of modes of the system.

The transfer function can be rewritten in a pole-residue form or the so-called “modal” model (assuming all poles have multiplicity one):

$$\alpha(s) = \sum_{r=1}^N \left( \frac{\mathbf{R}_r}{s - \lambda_r} + \frac{\mathbf{R}_r^*}{s - \lambda_r^*} \right) \quad (7)$$

The residue matrices  $\mathbf{R}_r$  are given by:

$$\mathbf{R}_r = \lim_{s \rightarrow \lambda_r} (\alpha(s)(s - \lambda_r)) \quad (8)$$

With

$$\alpha_{ij}(s) = \sum_{r=1}^N \left( \frac{{}_r R_{ij}}{s - \lambda_r} + \frac{{}_r R_{ij}^*}{s - \lambda_r^*} \right) \quad (9)$$

The elements of FRF are found by letting  $s = j\omega$  (when displacement is the response parameter, FRF is called a 'Receptance FRF' and is usually written as  $\alpha(\omega)$ ):

$$\alpha_{ij}(j\omega) = \sum_{r=1}^N \left( \frac{{}_r R_{ij}}{j\omega - \lambda_r} + \frac{{}_r R_{ij}^*}{j\omega - \lambda_r^*} \right) \quad (10)$$

The equivalent non-factorized (polynomial) form is given by:

$$\alpha_{ij}(j\omega) = \sum_{r=1}^N \frac{{}_r A_{ij}}{\omega_r^2 - \omega^2 + 2j\zeta_r \omega \omega_r} = \sum_{r=1}^N \frac{\phi_{ir} \phi_{jr}}{\omega_r^2 - \omega^2 + 2j\zeta_r \omega \omega_r} \quad (11)$$

$$\mathbf{A}_r = \begin{Bmatrix} \phi_1 \\ \phi_2 \\ \vdots \\ \phi_N \end{Bmatrix}_m [\phi_1 \ \phi_2 \ \dots \ \phi_N]_m \quad (12)$$

Where  $\phi_1, \phi_2, \dots$  are modal constants. These are scaled (or mass –normalized) modal constants. In experimental modal testing, modal constants  ${}_r A_{ij}$  are estimated from the measured FRF data.

Here  $\lambda_m$  is the complex frequency (Eigen value) of the  $m^{th}$  mode:

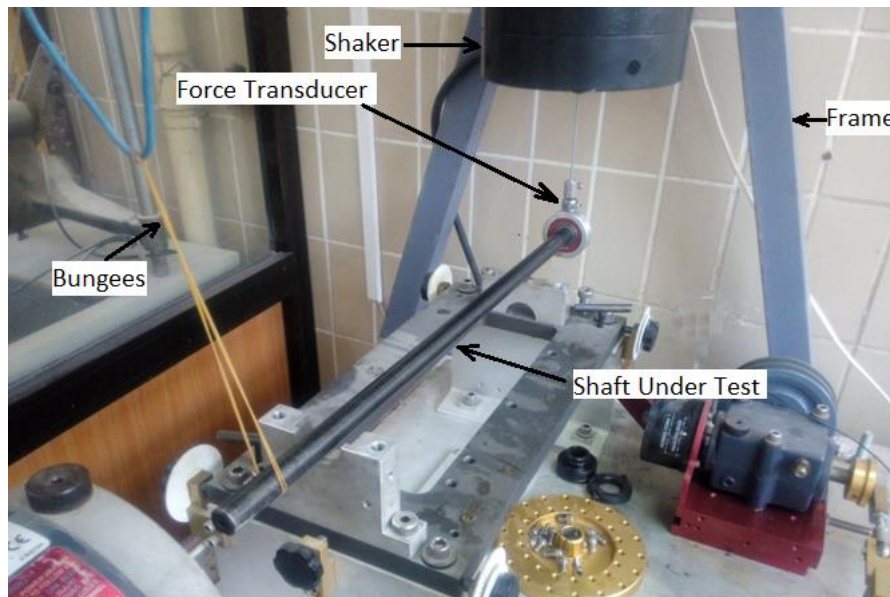
$$\lambda_r = -\zeta_r \omega_r + j \sqrt{1 - \zeta_r^2} \omega_r = -\sigma_r + j\omega_{d,r} \quad (13)$$

with  $f_d = \omega_d/2\pi$  the damped natural frequency,

$f_n = \omega_n/2\pi$  the (undamped) natural frequency where  $\omega_n = |\lambda|$ , and

$\zeta = c/2m\omega_n = \sigma/|\lambda|$  the damping ratio ( $f_d = f_n \sqrt{1 - \zeta^2}$ ).

Figure 1 shows the arrangement of the structure and the shaft under modal testing. The shaft is hanged by soft bungees to ensure ideal free-free boundary conditions in horizontal position. Heavy and rigid frame is used to minimize the transmission of forces between the excited shaft and foundation.



**Figure 1.** Experimental set up.

Commonly, there are two ways to apply excitation force on tested structure:

#### 4.1. Impact Hammer

Used to excite the structure by impulse force. Ideal Impact means ideal impulse force, which is in turn motivate largest number of vibrational modes with equal energy.

Force sensor is fixed to the end of the impact hammer to measure and record the force. Hard tip is fitted to the hammer used in this work to excite wider range of frequencies. Brüel & Kjaer Type 8200 force transducer is used to collect impact force data, while Brüel & Kjaer Type 4366 with mass of 26 g vibration transducer (piezoelectric accelerometer) is used to collect the dynamic response data (hence, it is so called “Instrumented Hammer”). The frequency response function was generated at a host notebook computer using SigTool software. Modal parameters are extracted from generated FRFs using ME’scope software, utilizing its MDOF curve-fitting tool.

#### 4.2. Shaker

It is electrical device used as source of force to excite the structure at single point as impact hammer do. Prepared and amplified input signal (sinusoidal, sweep-sine, or random signal in a specified frequency band) fed to shaker. In this work, Brüel & Kjaer Type 4808 vibration exciter (shaker) is utilized.

Coherence function  $\gamma(\omega)$  is an important indicator of linear relationship between excitation and response signals, defined as:

$$\gamma^2(\omega) = \frac{|G_{FX}(\omega)|^2}{G_{FF}(\omega) G_{XX}(\omega)} \quad (14)$$

Where  $G_{FF}$  and  $G_{XX}$  are auto spectrum of the excitation and response signals respectively, whilst  $G_{FX}$  is cross spectrum of these signals. Coherence value varies from zero to one. One means perfect linear relationship and noise-free signals, whilst zero means no relationship [13].

$$0 \leq \gamma^2(\omega) \leq 1 \quad (15)$$

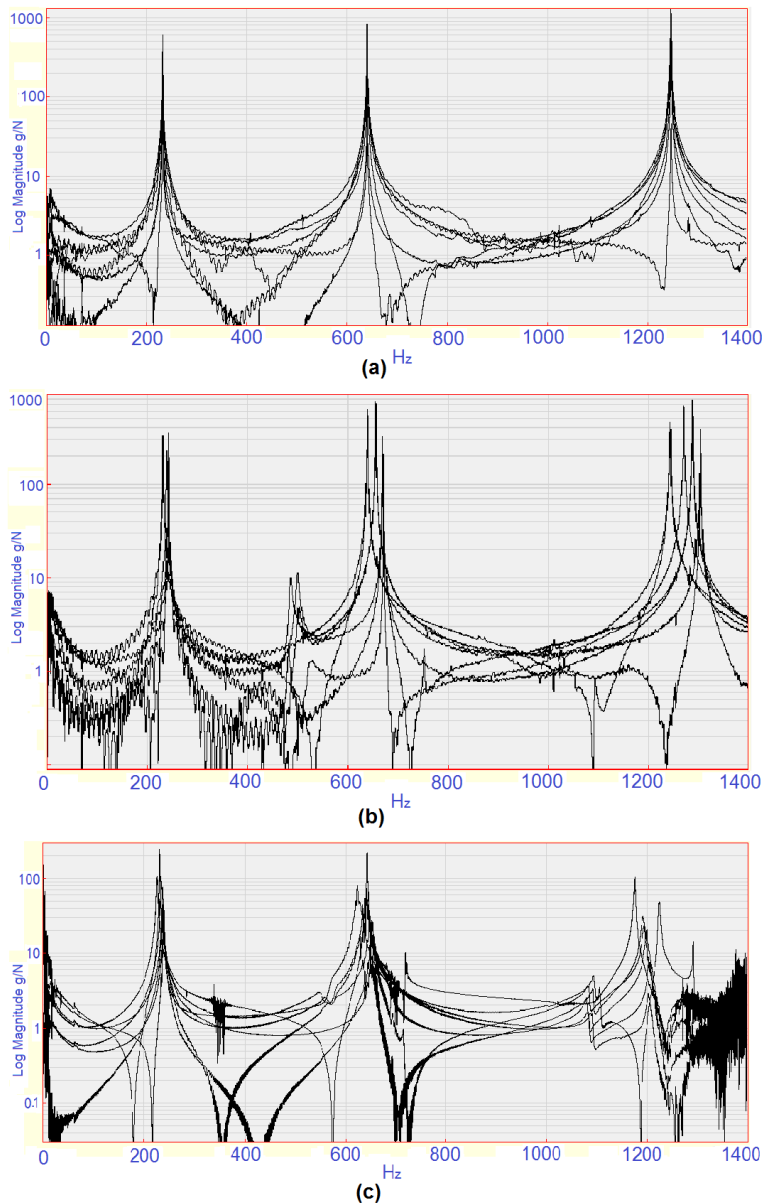
Also, coherence with one sample record and no averaging is always equal to 1. Hence, when performing impact test, more than one impact sample should be recorded, otherwise this function has no useful information. Nonlinearities and presence of noise lessen coherence value lower than one.

## 5. RESULTS AND DISCUSSION:

### 5.1. Shaft without disks

Depending on material properties and dimensions of the shaft stated above, the first three natural frequencies and mode shapes can be found from equations 1 and 2 respectively, and considered as analytical results. ANSYS software is utilized to perform numerical analysis task, to give natural frequencies and mode shapes.

Experimental modal analysis is done in three ways. The first two related to impact hammer, which are roving hammer and roving accelerometer. The third is done by fixed shaker and roving accelerometer. In all of them, seven equally distance (100 mm) testing points are marked on the shaft. In these three ways, experimental results were based on single-input, single-output (SISO) analysis. Figure 2 shows seven generated FRFs for each way of excitation. In Figure 2(a) all FRFs engage perfectly in three common spikes, unlike those of roving accelerometer shown in Figures 2(b) and 2(c). Coincided peaks in impact roving hammer test, resulted from no change in geometry and mass distribution. On contrary, moving the location of accelerometer resulted different geometry and mass distribution causing separation in some peaks in each mode.



**Figure 2.** FRFs resulted from (a) impact-roving hammer (b) impact-roving accelerometer (c) shaker test.

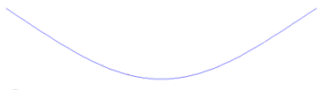
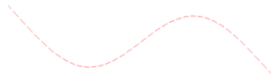

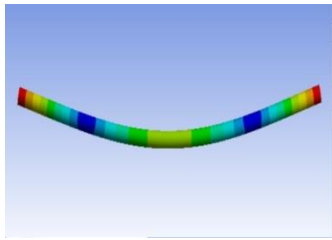
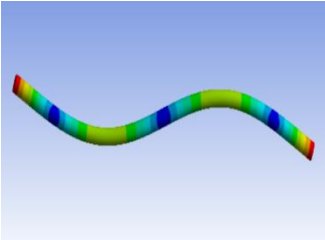
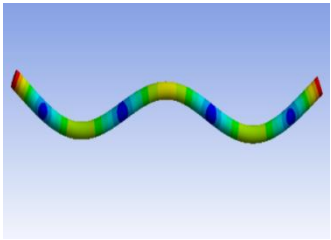
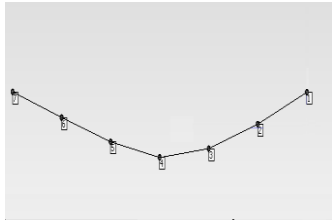
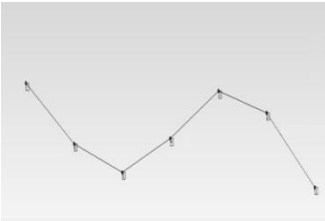
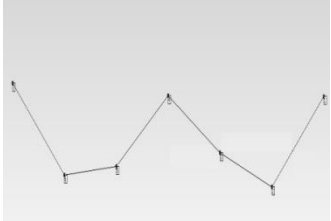
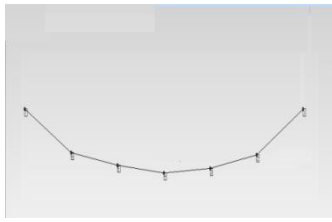
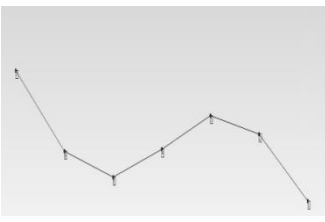
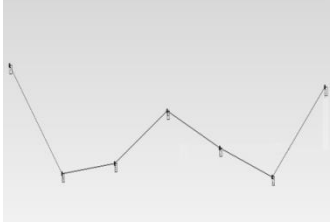
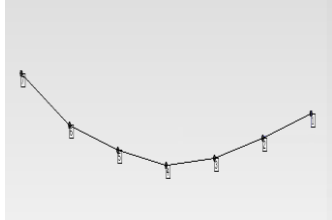
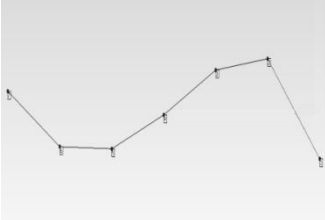
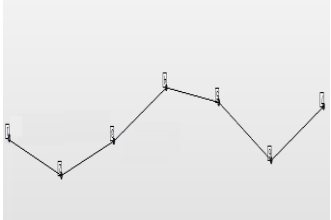
*Note:* In this work, shaker test performed by fixed position shaker and roving accelerometer.

Tables 2 and 3 show natural frequencies and mode shapes respectively of the first three modes resulted analytically, numerically, and experimentally.

**Table 2.** Natural frequencies [Hz] of three modes.

Method	1 <sup>st</sup> Mode	2 <sup>nd</sup> Mode	3 <sup>rd</sup> Mode
Analytical	237	654	1282
Numerical (ANSYS)	236	649	1263
Impact-Roving Hammer	233	641	1250
Experimental Impact-Roving Accelerometer	238	652	1270
Shaker	242	647	<b>1190</b>

**Table 3.** Fundamental three mode shapes of the shaft.

Method	1st Mode	2nd Mode	3rd Mode
Analytical			
Numerical (ANSYS)			
Experimental: Impact-Roving Hammer			
Experimental: Impact-Roving Accelerometer			
Experimental: Shaker			



For each individual mode, results in Table 2 are close, except that in 3<sup>rd</sup> mode from shaker test, which gave max deviation of 7 % from analytical solution.

Experimentally extracted modal damping ratios are listed in Table 4.

**Table 4.** Modal damping ratios.

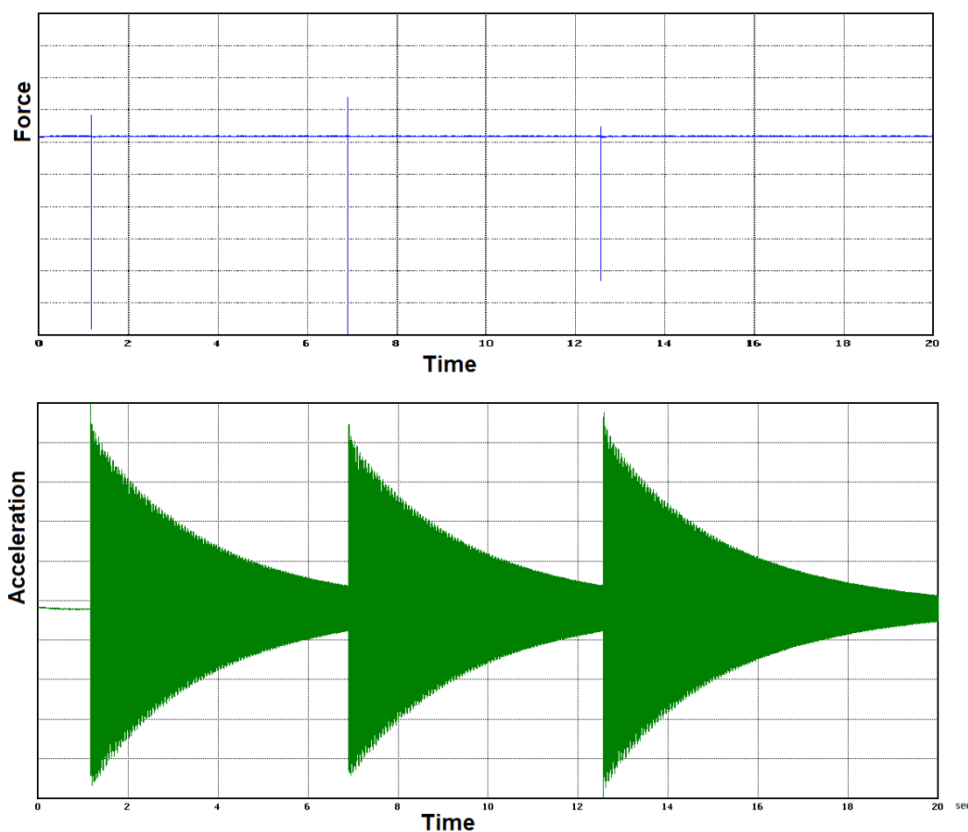
Method	$\zeta_1$ [%]	$\zeta_2$ [%]	$\zeta_3$ [%]
Impact-Roving Hammer	0.14	0.05	0.04
Impact-Roving Accelerometer	0.12	0.06	0.06
Shaker	0.22	0.06	0.15

As numbers in Table 3 indicate, damping ratio decreased at higher modes (except in 3<sup>rd</sup> mode of shaker test), but a common rule cannot be concluded, because in most cases, damping estimation is uncertain and engineers judgment dependent [14,15].

Mode shapes graphed experimentally are not smooth as those found analytically and numerically. This is because that experimental mode shapes based on discrete test points. Smoother shapes can be obtained by increasing reasonably number of test points.

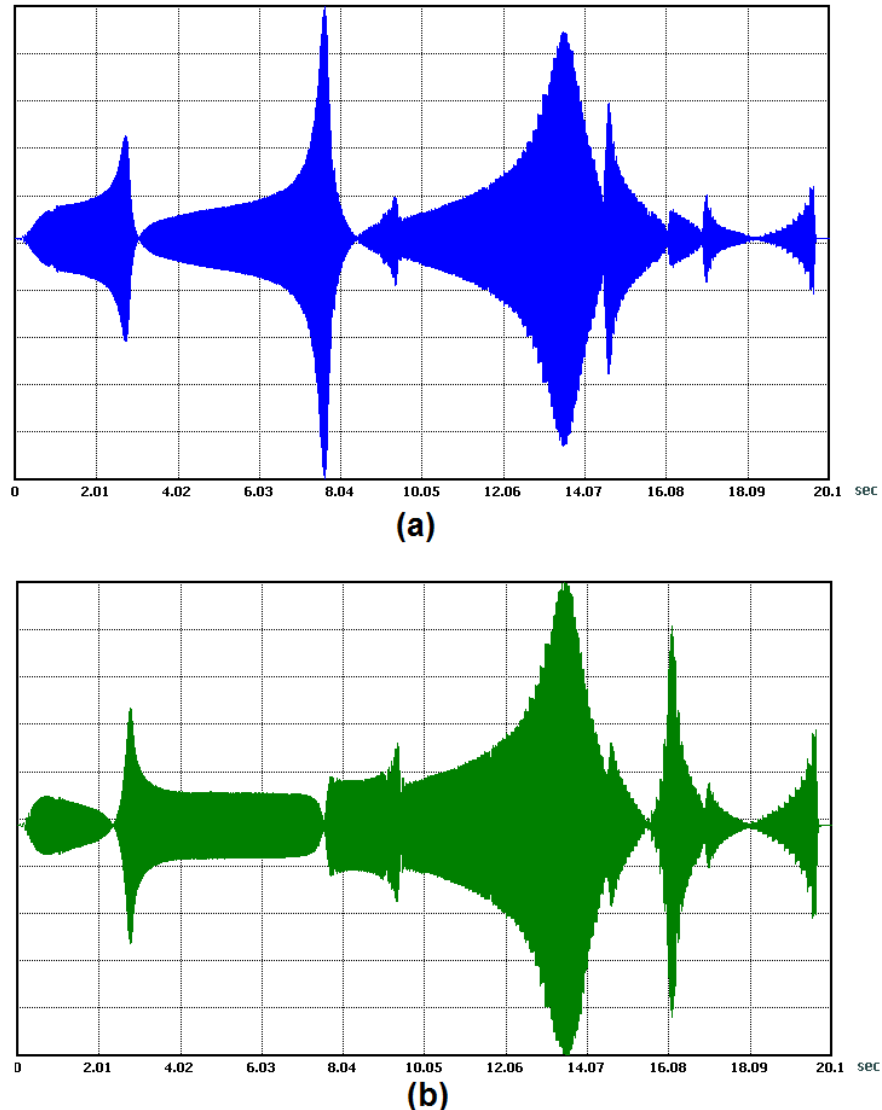
It is worth mentioning to express important DSP tool used in EMA. Windows are meant, which are mostly different when applied in impact test and shaker test. Windows types and basis are discussed in the literature extendedly [16,12].

In this work, three impacts were adopted for averaging, with sample time of 4.57 seconds for each. Figure 3 shows these impacts and the resulted responses.



**Figure 3.** (a) Three impacts (b) Resulted responses.

In shaker test, rectangular windows (no data modification) are suitable to give good results when applied on both excitation and response signals. Sinusoidal chirp (sweep) excitation was used in the test. This chirp starts at 5 Hz and ends at 1400 Hz, to cover the frequency range of interested modes. Figure 4 show shaker excitation and response signals.

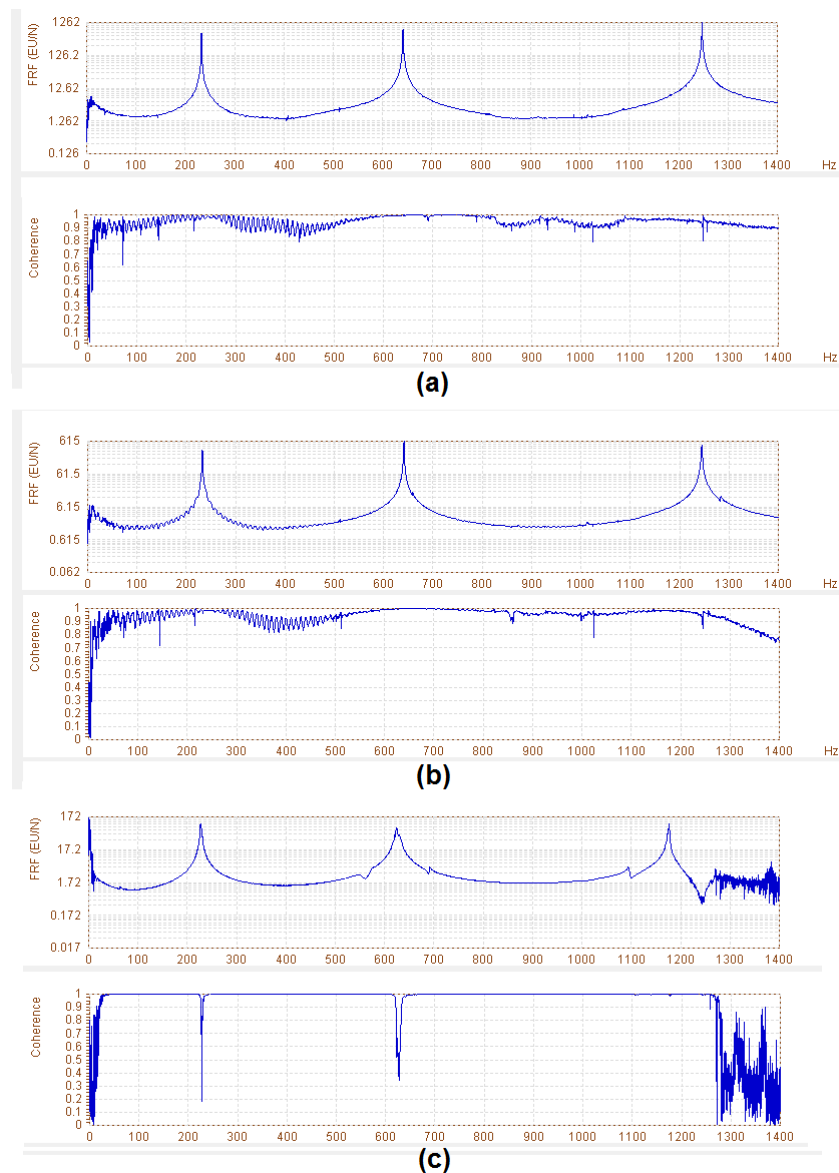


**Figure 4.** (a) Input chirp signal force applied on point No.1 (end point) on the shaft (b) Output acceleration from the same point.

*Note: Special case named “drive point” adopted in Figure.4, where input and output signals measured in the same location (point No.1 chosen in this case). This measurement symbolized as  $h_{11}$ , and has some important characteristics [3].*

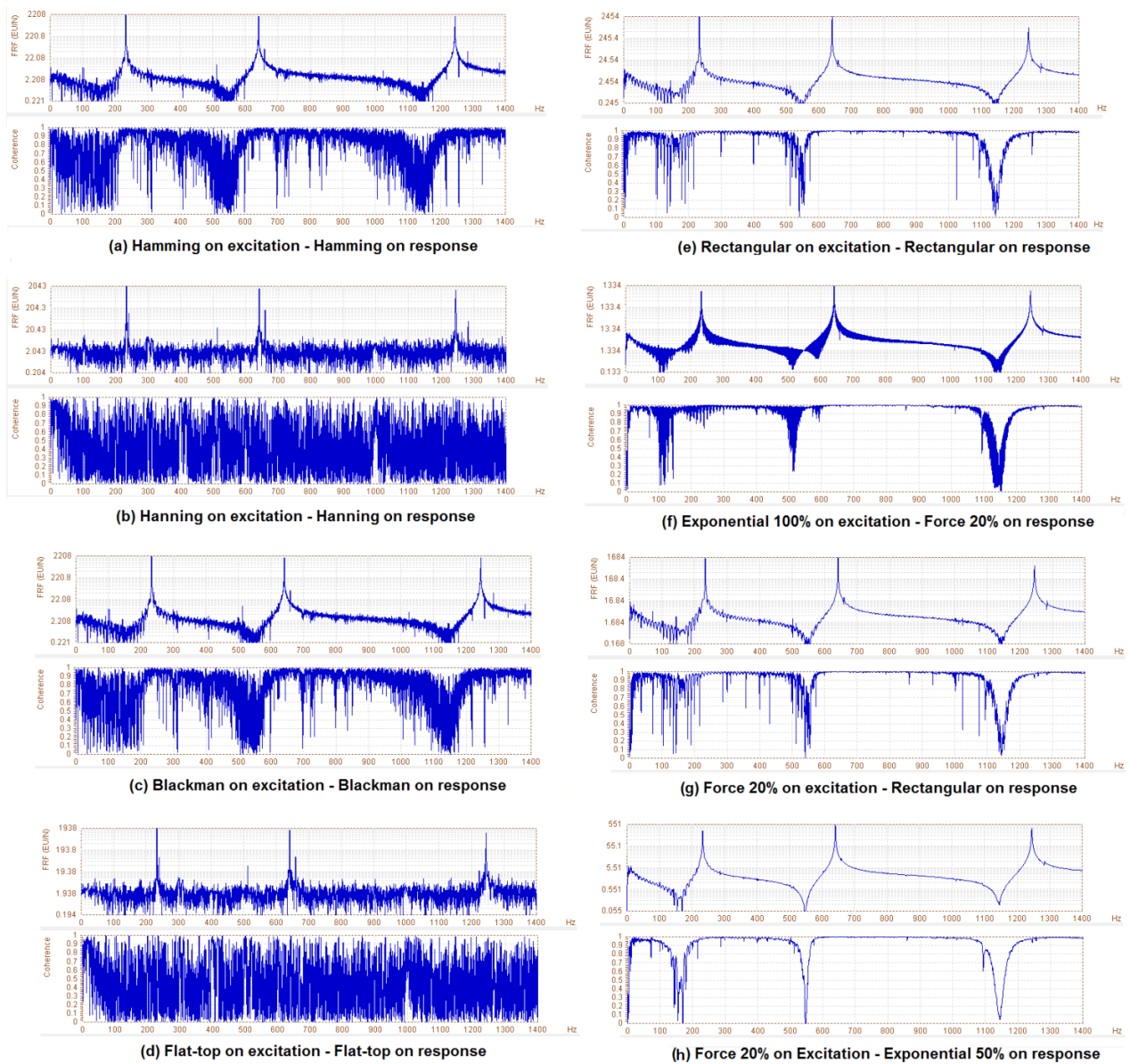
Figure.5 shows resulting FRFs and coherence functions when exciting point 1 (in three different ways) and measuring the response at point 7.

In impact excitation, difficulty in controlling either the force level or the frequency range could affect the signal to noise ratio in the measurement, thus resulting in poor quality data. Using shaker with chirp signal gives excellent signal to noise ratio [3]. Best coherence existed in Figure.5(c). Relatively less quality coherence resulted from impact tests.



**Figure 5.** FRF and coherence when exciting point 1 and measuring response from point 7. (a) impact-roving hammer (b) impact-roving accelerometer (c) shaker.

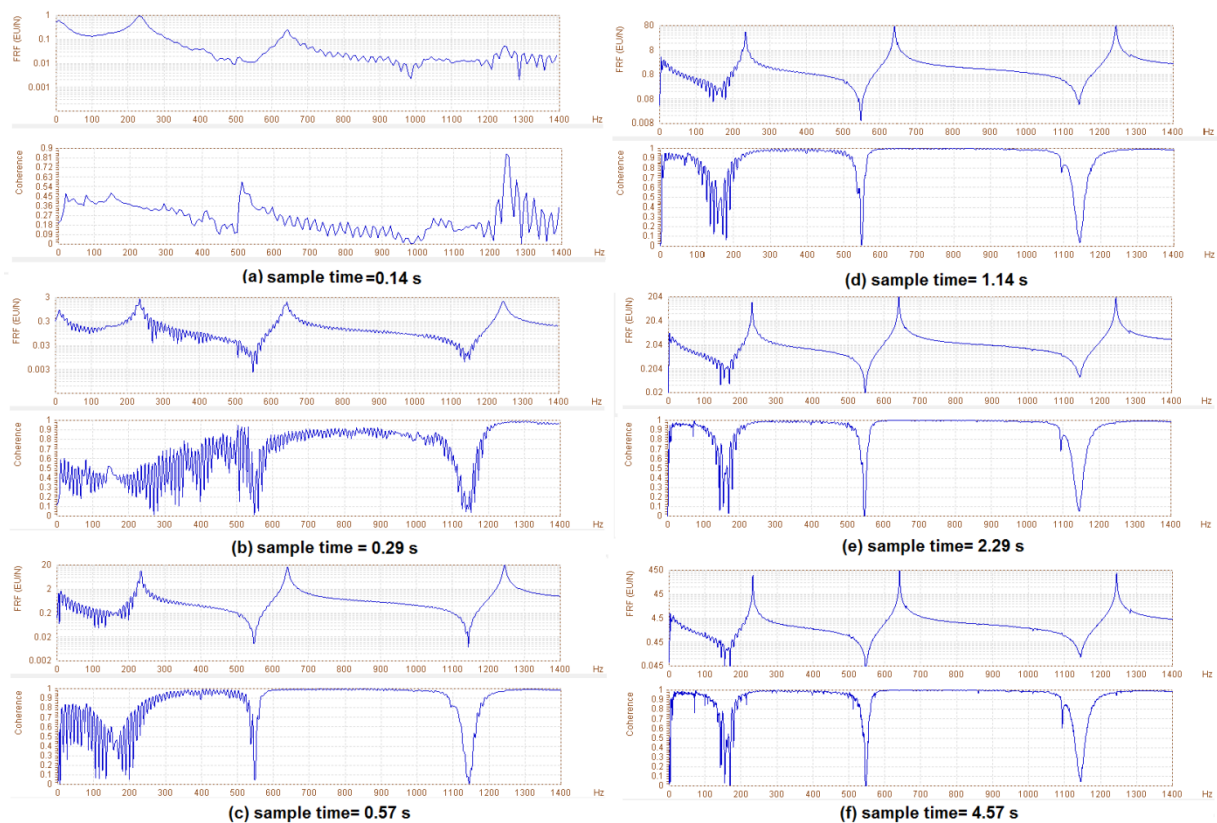
Implementing EMA requires wise selection of windows functions. Among many, seven well-known types of windows (which are: Hamming, Hanning, Blackman, Flat-top, Rectangular, Force, and exponential) are selected and applied on impact force and response signals. Figure 6 shows the effect of choosing windows on FRF and coherence function. Clearly, high quality FRF and mostly near-one coherence function obtained when applying force window on impact force signal and exponential window on response.



**Figure 6.** Effect of windows on FRF quality and coherence function.

*Note: Different combinations of windows (e.g. Force20%-rectangular, Hamming-Hanning, Hamming-Exponential 50%...etc.) are tested but not included here for brevity.*

Sample time for each impact is another important factor should be selected carefully. Figure 7 shows FRF and coherence plots for different values of sample time. As seen, longer sample (record) time considerably enhances FRF and coherence, hence ensures accurate estimation of modal parameters.



**Figure 7.** Effect of impact sample (record) time on FRF quality and coherence.

### 5.2. Shaft with two disks case

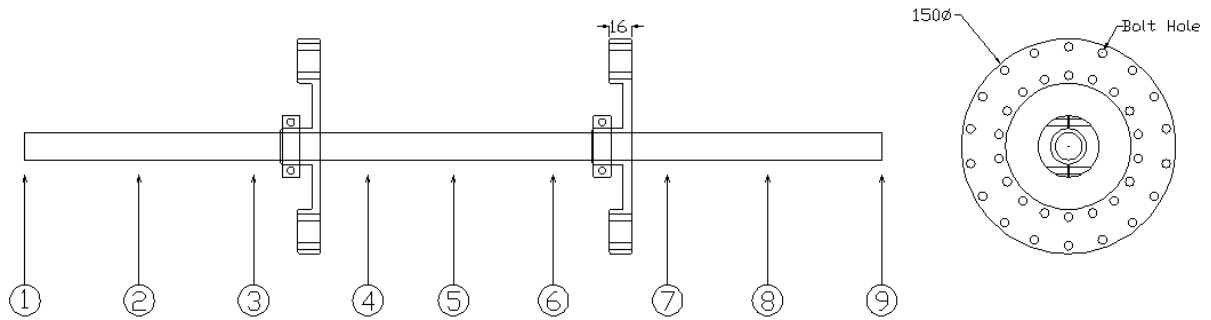
Figure 8 shows two 36-bolt holes disks attached to the same shaft tested above, while in Figure 9 a schematic drawing for this assembly. It is required to find the fundamental three natural frequencies and related mode shapes.

Experimental results are obtained by roving hammer impact test. Nine testing points on the shaft are selected in unequally distance scheme to avoid impacting on the disks, as shown in Figure 9. Disks are made of Aluminum, and two-piece shaft collars are used to fix the disks on the shaft.

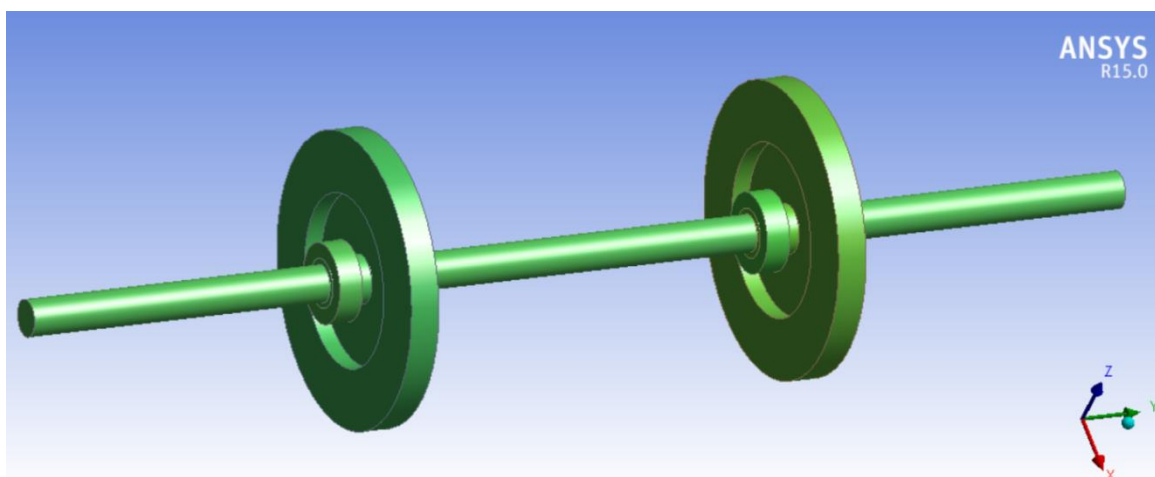
Numerical results are obtained by simulating the rotor (shaft-disks assembly) in ANSYS software as shown in Figure 10. In order to obtain the dynamic properties and behaviour of this case (and similar cases), it is found that the dominating factor is the selection of interface elements type in contact area between the disks and shaft. Here, disks are not bonded with shaft, so, the contact should be described as *Rough* type, which means no slipping and ensures possibility of separation of surfaces during vibration. This is the best description of this highly nonlinear behaved structure, and the results shown in Tables 5 and 6 are evidence.



**Figure 8.** Rotor assembly: shaft, disks, two-piece shaft collars.



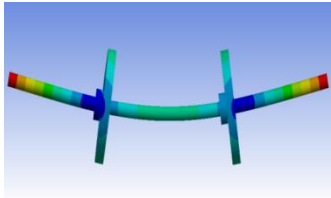
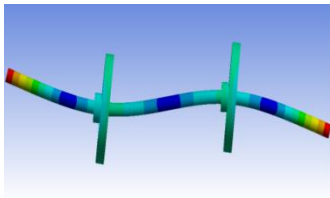
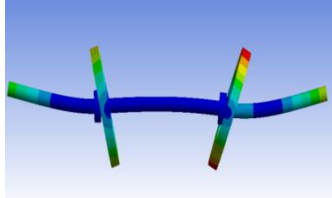
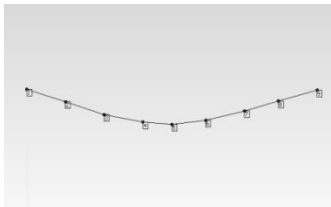
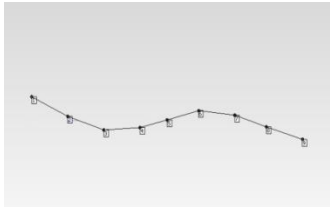
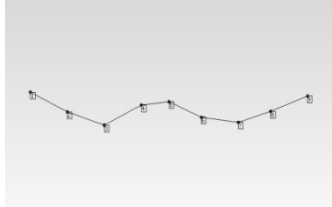
**Figure 9.** Schematic diagram of the rotor and nine testing points.



**Figure 10.** Simulation of the rotor in ANSYS software.



**Table 5.** Fundamental three mode shapes of the disks-shaft assembly.

Method	1st Mode	2nd Mode	3rd Mode
Numerical: ANSYS			
Experimental: Impact-Roving Hammer			

**Table 6.** Natural frequencies [ $H_z$ ] of three modes.

Method	1 <sup>st</sup> Mode	2 <sup>nd</sup> Mode	3 <sup>rd</sup> Mode
Numerical (ANSYS)	206	435	615
Experimental (Impact-Roving Hammer)	202	427	624
Error [%]	2	2	1.5

## 6. Conclusions

In this work, fundamental three natural frequencies of circular shaft has been found analytically, numerically, and experimentally by three EMA ways (i.e. impact roving hammer, impact roving accelerometer, and shaker roving accelerometer). Close natural frequency values and acceptable deviation from analytical results are found. Mode shapes were extracted from the five excitation methods and graphed. Similarity is evidence. Thus, high efficiency of EMA has been verified. Modal damping ratio is estimated experimentally for each mode.

Signals from shaker test have the best signal to noise ratio, unlike those noise contaminated in impact hammer tests, as evidenced by coherence plots. Windows and some other DSP settings are specified in this work, to be a reference for high quality and reliable results in similar tests.

As a further examination of EMA efficiency, two Aluminum 36-bolt holes disks are attached on the shaft by two-piece shaft collars. By these additions and by the nature of contact between the shaft and disks, the structure behaviour became highly nonlinear. In spite of this, EMA gave results that are close to the numerical values obtained by ANSYS with max percentage error of 2%.

**7. References:**

- [1] Kennedy C C and Pancu C D P. Use of Vectors in Vibration Measurement and Analysis. *J. Aero. Sci.*, 14(11) 1947.
- [2] Richard C and James M. Proper Use of Weighting Functions for Impact Testing. Proceedings of the Third International Modal Analysis Conference, Orlando, Florida, USA 1985.
- [3] Peter Avitabile: *Modal Testing A Practitioner's Guide*. First edition, John Wiley & Sons 2018.
- [4] Manoj Chouksey, Jayanta K Dutt and Subodh V Modak: Experimental modal analysis studies for spinning rotor-shaft system. VIII International Conference on Vibration Engineering and Technology of Machinery, Gdansk, Poland, 2012.
- [5] Songmao C, Alessandro S, and Christopher N: Estimation of the Dynamic Focused Ultrasound Radiation Force Generated by an Ultrasonic Transducer. Proceedings of the 35th IMAC, A Conference and Exposition on Structural Dynamics 2017 (pp.15-22).
- [6] Morteza H Sadeghi, Soheil Jafari and Bahman Nasserolelami: Modal Analysis of a Turbo Pump Shaft: An Innovative Suspending Method to Improve the Results. *IUST International Journal of Engineering Science*, vol.19, No.5-1, (2008). pp: 143-149.
- [7] Luis A, Eloy E, Helen J, Israel M, Hugo G. and José C: Dynamic model for high-speed rotors based on their experimental characterization. *IEEE Conf. Proc.* 2016.
- [8] Pramod K, Sankha B and Arbind K: An Experimental Study of Modal Parameter of Cantilever Beam with Various Cracked Condition. *International Journal for Research in Applied Science & Engineering*. Volume 4 Issue III, March 2016.
- [9] J He and Z Fu: *Modal analysis*, Butterworth-Heinemann, Oxford, England, 2001.
- [10] Mohammad Reza Ashory: *High Quality Modal Testing Methods*. PhD Thesis, Imperial College, University of London, 1999.
- [11] Robert D Blevins: *Formulas for Dynamics, Acoustics and Vibration*. John Wiley & Sons, 2016.
- [12] D J Ewins: *Modal Testing: Theory and Practice*. John Wiley & Sons, Exeter, UK, 1995.
- [13] Alena Bilošová: *Modal Testing*. Ostrava 2011.
- [14] Brincker R, Zhang L and Andersen P: Output-Only Modal Analysis by Frequency Domain Decomposition. Conference on Noise and Vibration Engineering 2000, (pp. 717-723), Leuven.
- [15] Nathalie Labonnote and Kjell Arne Malo: Damping measurements in timber beams using impact testing. Proceedings of the 8th International Conference on Structural Dynamics, EURO DYN 2011. pp.1097-1101.
- [16] Fladung W A: Windows Used for Impact Testing. Proceedings, SEM-IMAC, 1997.